ISSN 1070-3284, Russian Journal of Coordination Chemistry, 2020, Vol. 46, No. 11, pp. 762–771. © Pleiades Publishing, Ltd., 2020.
Russian Text © The Author(s), 2020, published in Koordinatsionnaya Khimiya, 2020, Vol. 46, No. 11, pp. 668–697.

Heterometallic Complexes Based on Triphenylantimony(V) Quinone-Catecholate

L. S. Okhlopkova[a], I. V. Smolyaninov[b], and A. I. Poddel'skii[a, *]

[a] *Razuvaev Institute of Organometallic Chemistry, Russian Academy of Sciences, Nizhny Novgorod, 603137 Russia*
[b] *Southern Research Center, Russian Academy of Sciences, Rostov-on-Don, 344006 Russia*
**e-mail: aip@iomc.ras.ru*

Received May 4, 2020; revised June 10, 2020; accepted June 17, 2020

Abstract—Heterometallic chromium(III) $Cr^{III}[(SQ\text{-}Cat)SbPh_3]_3$ (**I**), copper(II) $Cu^{II}[(SQ\text{-}Cat)SbPh_3]_2$ (**II**), and zinc $I_2Zn(Q\text{-}Cat)SbPh_3$ (**III**) and $IZn(SQ\text{-}Cat)SbPh_3$ (**IV**) complexes, where SQ is the corresponding *o*-semiquinone radical anion, and Cat is the catecholate dianion (mono- and direduced forms of the quinone fragment), are synthesized on the basis of the mononuclear triphenylantimony(V) quinone-catecholate complex $(Q\text{-}Cat)SbPh_3$, which was derived from 4,4'-di-(6-*tert*-butyl-3-methylbenzo-1,2-quinone) (Q-Q). The one-electron oxidation and one-electron reduction of chromium complex **I** afford the paramagnetic derivatives $[Cr^{III}[(Q\text{-}Cat)SbPh_3][(SQ\text{-}Cat)SbPh_3]_2]^+$ ($\mathbf{I}^+$) and $[Cr^{III}[(Cat\text{-}Cat)SbPh_3][(SQ\text{-}Cat)SbPh_3]_2]^-$ ($\mathbf{I}^-$), respectively, which are easily detected by EPR spectroscopy. The EPR spectroscopy data and measurements of the temperature dependence of the magnetic susceptibility of copper complex **II** indicate in favor of the localization of the lone electron on the organic ligand, which can be explained by the antiferromagnetic metal–ligand exchange in this complex (J(SQ-Cu) = −157 cm^{-1}, J(SQ-SQ) = −10.0 cm^{-1}). The coordination of $(Q\text{-}Cat)SbPh_3$ as neutral *o*-quinone to zinc iodide with the formation of complex **III** increases significantly the oxidation ability of the quinone fragment in this complex (E^{Red1} = 0.43 V for **III** and −0.45 V for $(Q\text{-}Cat)SbPh_3$ vs. Ag/AgCl/KCl(sat.)), and the complex can oxidize the iodide anion to iodine with the formation of paramagnetic derivative **IV**, whose EPR spectrum is characteristic of complexes of the M(SQ-Cat) type. The redox properties of complexes **I** and **III** are studied by cyclic voltammetry.

Keywords: redox-active ligand, catecholate, heterometallic complex, antimony, EPR

DOI: 10.1134/S1070328420110068

INTRODUCTION

Numerous attempts to imitate both the structure and function of some enzymes for the use in diverse areas from catalytic synthesis of fuel cells to solar energy capture and storage are evoked due to high interest in many chemical and biochemical processes mediated by the heterometallic compounds and enzymes [1–7]. Significant attention is given to the interaction between various metals and metal-containing organic fragments in the synthetic heterometallic complexes and the influence of these interactions on the electronic structures, redox-active properties, electron transfer, and reactivity. The complexes based on bis-*o*-quinones which are able to bind two and more different metallic centers and being redox-active ligands capable of reversible adding one or several electrons represent an interesting area of research. This considerably extends the range of redox properties of the formed compounds and also results in the possibility of obtaining combinations of oxidation states of the metal(s) and reduction states of the redox-active ligands [8–16].

EPR spectroscopy is an important and informative method for studying paramagnetic coordination compounds containing paramagnetic metal ions and radical species, since EPR provides a useful information about the structure of the coordination node and mutual arrangement of the ligands in the coordination sphere of the metal and also allows one to study the dynamic processes occurring with a change in the geometry of the complexes. Since in the redox series of *o*-quinones one of the reduced forms, namely, *o*-semiquinone, is paramagnetic, EPR spectroscopy can provide an important information about the structures and chemical properties of the *o*-semiquinone and related complexes in many cases [17–21]. The EPR method is also informative for the bis-*o*-benzoquinone derivatives [12–26]. We have previously synthesized the triphenylantimony(V) catecholate complex $(Q\text{-}Cat)SbPh_3$ based on 4,4'-di-(6-*tert*-butyl-3-methylbenzo-1,2-quinone) (Q-Q) [27]. The complex of Q-Q was shown to be capable of forming *o*-semiquinone derivatives of the $M(SQ\text{-}Cat)SbPh_3$ type [24].

The heterometallic *o*-semiquinone complexes of chromium(III) $Cr^{III}[(SQ\text{-}Cat)SbPh_3]_3$ (**I**) and cop-

per(II) $Cu^{II}[(SQ\text{-}Cat)SbPh_3]_2$ (**II**), as well as zinc derivatives of the $I_2Zn(Q\text{-}Cat)SbPh_3$ (**III**) type with the neutral coordinated *o*-quinone fragment and its *o*-semiquinone derivative $IZn(SQ\text{-}Cat)SbPh_3$ (**IV**) were studied in this work.

EXPERIMENTAL

Synthesis, isolation, and study of the properties of the complexes were carried out in evacuated ampules without oxygen. The organic solvents used in the work were purified using standard procedures [28]. The starting $(Q\text{-}Cat)SbPh_3$ was synthesized using a described method [27].

Synthesis of tris[(4-(3-methyl-6-*tert*-butylbenzosemiquinolate-1,2)-3-methyl-6-*tert*-butylcatecholato)triphenylantimony(V)]chromium(III) $Cr^{III}[(SQ\text{-}Cat)SbPh_3]_3$ (I). A solution of $(Q\text{-}Cat)SbPh_3$ (100 mg, 0.14 mmol) in THF (25 mL) was stirred for 20 min with thallium amalgam excess. The color of the solution changed from cherry to yellow-green. The solution was carefully decanted from the amalgam, and the second portion of $(Q\text{-}Cat)SbPh_3$ (100 mg, 0.14 mmol) in THF (20 mL) was added to the solution with vigorous stirring. In 10 min, the obtained solution of thallium(I) semiquinolate $Tl(SQ\text{-}Cat)SbPh_3$ was mixed with a solution of chromium(III) chloride tetrahydrofuranate (35 mg, 0.093 mmol) in THF (20 mL). The formed precipitate of TlCl was filtered off from the reaction mixture. Then THF was removed, and the residue was dissolved in toluene. The resulting solution was again filtered and concentrated. The formed finely crystalline violet product **I** was separated by filtration, washed with cold toluene, and dried in vacuo. The yield of complex **I** was 79%.

For $C_{120}H_{123}O_{12}CrSb_3$

Anal. calcd., %	C, 66.27	H, 5.66	Sb, 16.84
Found, %	C, 66.25	H, 5.65	Sb, 16.73

IR (ν, cm^{-1}): 1658 w, 1642 w, 1565 s, 1407 s, 1340 m, 1316 m, 1277 s, 1246 s, 1180 m, 1102 w, 1069 s, 997 m, 960 s, 891 w, 864 w, 821 w, 778 w, 730 s, 694 s, 629 w, 540 m, 455 m.

Bis[(4-(3-methyl-6-*tert*-butylbenzosemiquinolate-1,2)-3-methyl-6-*tert*-butyl-catecholato)triphenylantimony(V)]copper(II) $Cu^{II}[(SQ\text{-}Cat)SbPh_3]_2$ (II) was synthesized by a method similar to that for complex **I** using $CuCl_2$ (19 mg, 0.14 mmol) and $(Q\text{-}Cat)SbPh_3$ (200 mg). The yield of finely crystalline complex **II** was 75%.

For $C_{80}H_{82}O_8CuSb_2$

Anal. calcd., %	C, 64.97	H, 5.55	Sb, 16.51
Found, %	C, 65.00	H, 5.61	Sb, 16.53

IR (ν, cm^{-1}): 1403 m, 1303 m, 1244 w, 1213 w, 1169 w, 1139 w, 1062 m, 1039 m, 960 m, 893 w, 863 w, 820 w, 771 w, 727 w, 694 w, 676 m, 626 w, 560 w, 512 w.

Synthesis of *O,O'*-[4-(2-methyl-5-*tert*-butylcyclohexadiene-1,5-dion-3,4-yl)-3-methyl-6-*tert*-butyl-catecholato)triphenylantimony(V)-diiodozinc $I_2Zn(Q\text{-}Cat)SbPh_3$ (III). A freshly prepared solution of zinc iodide (44.6 mg, 0.14 mmol) in toluene was poured to a toluene solution of $(Q\text{-}Cat)SbPh_3$ (100 mg, 0.14 mmol). The color of the solution immediately changed from cherry to violet. After the solution was concentrated and kept at room temperature for 3 h, a violet finely crystalline product was formed, which was filtered off and dried under reduced pressure. The yield of complex **III** was 65%.

For $C_{40}H_{41}O_4I_2SbZn$

Anal. calcd., %	C, 46.78	H, 4.00	Sb, 11.89
Found, %	C, 46.75	H, 4.05	Sb, 11.90

IR (ν, cm^{-1}): 1363 s, 1291 s, 1274 s, 1246 m, 1212 s, 1140 s, 1050 s, 963 s, 929 w, 866 w, 818 w, 730 s, 671 s, 622 w, 560 w, 511 w, 484 w, 468 w.

Synthesis of [(4-(3-methyl-6-*tert*-butylbenzosemiquinolate-1,2)-3-methyl-6-*tert*-butyl-catecholato)triphenylantimony(V)]iodozinc $IZn(SQ\text{-}Cat)SbPh_3$ (IV). A blue-violet finely crystalline product was obtained from the mother liquor remained after the isolation of complex **III**, which was cooled and kept at 0°C for 2 days. The yield of complex **IV** was 15%.

For $C_{40}H_{41}O_4IZnSb$

Anal. calcd., %	C, 53.39	H, 4.56	Sb, 13.57
Found, %	C, 53.35	H, 4.55	Sb, 13.59

IR (ν, cm^{-1}): 1612 m, 1591 m, 1575 m, 1500 m, 1336 s, 1298 s, 1278 s, 1242 s, 1217 m, 1184 m, 1141 m, 1063 m, 996 m, 963 m, 862 w, 819 w, 735 s, 689 s, 624 w, 562 w, 521 w, 504 w, 454 s.

IR spectra were recorded on an FSM 1201 FT-IR spectrometer in Nujol. The electronic absorption spectra of the complexes were detected on Perkin Elmer UV/VIS Lambda 25 spectrophotometers in a range of 280–1100 nm (quartz cells, absorbing layer thickness 10 mm) at 298 K. Elemental analysis was carried out on a Euro EA 3000 C,H,N analyzer and also by the pyrolytic decomposition method in an oxygen flow. Quantum chemical calculations were performed using the Gaussian09 program package [29] with the B3LYP/def2tzvp calculation procedure. The static magnetic susceptibility of the samples was measured on an MPMS-5S SQUID magnetometer (magnetic field intensity 0.5 T) in a temperature range of 2–330 K at the International Tomography Center (Siberian Branch, Russian Academy of Sciences, Novosibirsk, Russia). The magnetic properties of the com-

plexes were simulated and the exchange interaction parameters between the paramagnetic centers were determined using the Mjollnir program [30]. EPR spectra were recorded on a Bruker EMX EPR spectrometer (working frequency ~9.7 GHz). Diphenylpicrylhydrazyl (DPPH, $g = 2.0037$) was used as a standard when determining the g factor. EPR spectra were simulated using the WinEPR SimFonia program (Bruker). Oxidation potentials were measured by cyclic voltammetry (CV) in a three-electrode cell on an IPC-pro potentiostat in argon. A stationary glassy carbon (GC) electrode with a diameter of 2 mm served as the working electrode, a platinum plate ($S = 18$ mm^2) was the auxiliary electrode, and Ag/AgCl/KCl(sat.) with a water-proof membrane was used as the reference electrode. The potential sweep rate was 0.2 V/s. Electron ionization mass spectra were measured using a MALDI-Toff time-of-flight mass spectrometer with the DCTB matrix.

RESULTS AND DISCUSSION

The quinone-catecholate complex (Q-Cat)$SbPh_3$ [27], being a convenient basis for the preparation of the heterometallic compounds [24], has previously been synthesized at the Razuvaev Institute of Organometallic Chemistry (Russian Academy of Sciences) [27]. The exchange reaction between the *o*-semiquinone derivative M(SQ-Cat)$SbPh_3$ (M = Na, K, and Tl) and chromium(III) chloride should afford the corresponding chromium(III) tris-*o*-semiquinone derivative. Indeed, the reaction of the chromium(III) chloride tetrahydrofuranate in a THF solution with thallium *o*-semiquinolate based on (Q-Cat)$SbPh_3$, which was synthesized in situ, is accompanied by the instant change in the color of the reaction mixture (Scheme 1).

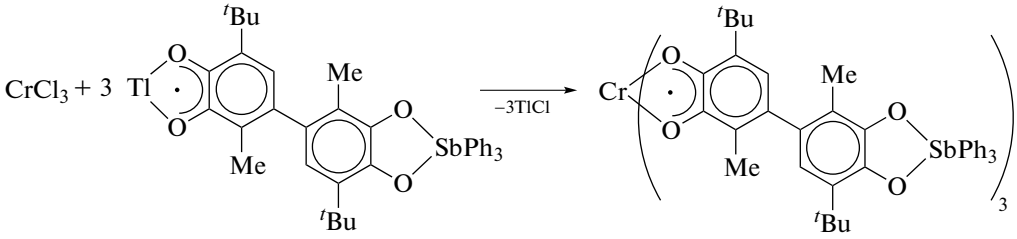

Tl^{I}(SQ-Cat)$SbPh_3$ $Cr^{III}[(SQ\text{-}Cat)SbPh_3]_3$ (**I**)

Scheme 1.

The product of the exchange reaction was a complex identified using elemental analysis, IR spectroscopy, and mass spectroscopy as tris(ligand) chromium derivative **I**.

The formation of complex **I** containing the ligand in the catecholate and semiquinone forms is confirmed by the characteristic set of bands in the IR spectrum in a range of 700–1600 cm^{-1}. The intense bands of stretching vibrations of the sesquialteral C–O bonds are observed in a range of 1350–1450 cm^{-1}, whereas stretching vibrations of the C–O ordinary bond are observed in a range of 1200–1300 cm^{-1}, confirming the mixed nature of the organoantimony fragment. The signals from the fragmentation (the major route of which is the cleavage of the C–C bond connecting two aryl rings) products are also observed in the mass spectrum of complex **I** along with the peak corresponding to the $[\mathbf{I}]^+$ molecular ion. Unfortunately, all attempts to isolate the crystals suitable for X-ray diffraction analysis were unsuccessful.

The oxidation of complex **I** with silver triflate in a molar ratio of 1 : 1 in a THF solution results in the one-electron oxidation of the complex to form the $[Cr^{III}[(Q\text{-}Cat)SbPh_3][(SQ\text{-}Cat)SbPh_3]_2]^+$ cation ($\mathbf{I}^+$). The initial complex has the singlet ground spin state due to the antiferromagnetic metal–ligand exchange between high-spin chromium(III) (d^3, $S = 3/2$) and three radical-anionic *o*-semiquinone centers ($S = 1/2$). A similar magnetic behavior was earlier demonstrated several times for other chromium(III) tris-*o*-benzosemiquinone complexes [31–33]. The one-electron oxidation results in the formation of paramagnetic derivative $\mathbf{I}^+$ with $S = 1/2$, whose isotropic EPR spectrum in a THF solution represents the signal with $g_{iso} = 1.9700$ and satellite splitting on the magnetic isotope of the chromium atom (^{53}Cr, $I = 3/2$, 9.5%) with the hyperfine coupling (HFC) constant $a_i(^{53}Cr) = 27.6$ G (Fig. 1a). These parameters are close to the parameters of the EPR spectrum of the chromium complex $[Cr(Cl_4BQ)(Cl_4SQ)_2]^+[SbF_6]^-$ ($g_{iso} = 1.969$, $a_i(^{53}Cr) = 27.5$ G) [34].

The EPR spectra of similar electron-transfer complexes based on chromium tris(tetrachloro(bromo)-*o*-semiuinolates and cobaltocene, tetrathiafulvalene have close characteristics [35].

The one-electron reduction of chromium complex **I** by metallic sodium in a THF solution results in the reduction of one of the *o*-benzosemiqui-

none ligands to the catecholate ligand due to which the paramagnetic derivative $Na^+[Cr^{III}[(Cat\text{-}Cat)SbPh_3][(SQ\text{-}Cat)SbPh_3]_2]^-$ (Na^+I^-) containing one lone electron is formed. The EPR spectrum of this derivative have somewhat different characteristics: $g_{iso} = 1.9725$ and $a_i(^{53}Cr) = 24.9$ G (Fig. 1b). A similar anionic chromium complex based on the 3,5-di-*tert*-butyl-*o*-benzosemiquinone ligands $K^+[Cr^{III}(3,5\text{-}DBCat)(3,5\text{-}DBSQ)_2]^-$ has the EPR spectrum with resembling characteristics: $g_{iso} = 1.972$ and $a_i(^{53}Cr) = 24.3$ G [36]. No additional hyperfine structure is observed on the magnetic nuclei of the ligands. The EPR spectral parameters indicate that the lone electron is localized on the orbital having a significantly metallic character (considerable contribution of the metal orbitals).

According to the CV data, three redox transitions are observed in the cathodic range for chromium derivative **I**: the first two transitions are quasi-reversible and one-electron, and the third peak is irreversible (Table 1).

The redox transitions detected in the cathodic range characterize the electroreduction of the *o*-semiquinone fragment of the ligand. Two irreversible multielectron oxidation peaks are detected for complex **I** in the anodic range at 1.00 and 1.29 V. The observed pattern can be explained by close potentials of the redox transitions Cat/SQ in the catecholate fragment of the $[(SQ\text{-}Cat)SbPh_3]^-$ ligand with the SQ/Q redox transition in the *o*-semiquinolate fragment of the ligand. The CV results of the initial $(Q\text{-}Cat)SbPh_3$ complex, where two irreversible reduction steps are observed at −0.45 and −0.62 V, are presented for comparison. The oxidation potentials of $(Q\text{-}Cat)SbPh_3$ and complex **I** are well consistent.

Copper complex **II** with the similar antimony-containing ligand was synthesized via a similar procedure (Scheme 2).

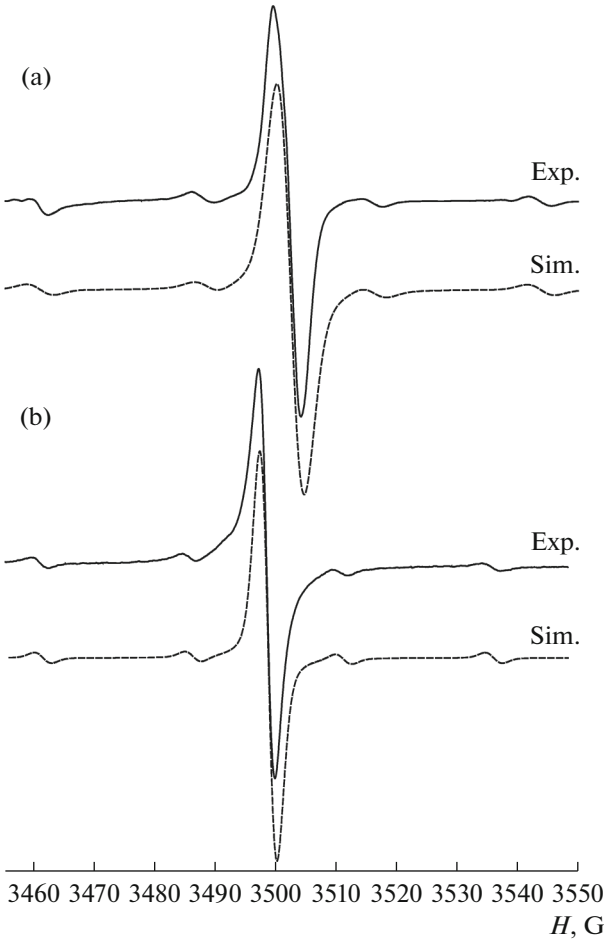

Fig. 1. EPR spectra of (a) $[Cr^{III}[(Q\text{-}Cat)SbPh_3][(SQ\text{-}Cat)SbPh_3]_2]^+[OTf]^-$ ($\mathbf{I}^+[OTf]^-$) and (b) $Na^+[Cr^{III}[(Cat\text{-}Cat)SbPh_3][(SQ\text{-}Cat)SbPh_3]_2]^-$ ($Na^+\mathbf{I}^-$): exp. is experimental (THF, 293 K), and sim. is computer simulation (WINEPR SimFonia 1.26).

Table 1. Redox potentials of complex **I** according to the CV data (CH_2Cl_2, GC electrode, 0.15 M Bu_4NClO_4, c = 0.002–0.003 mol/L, V = 0.2 V/s, vs. Ag/AgCl/KCl(sat.))

Complex	E^1_{pc}, V*	E^2_{pc}, V*	E^3_{pc}, V*	E^1_{pa}, V*	E^2_{pa}, V*
I	−0.09	−0.74	−1.15	1.00	1.29
III	0.43	−0.49		0.85	0.96
$(Q\text{-}Cat)SbPh_3$	−0.45	−0.62		1.10	1.40

* E^1_{pc} is the peak potential of the first cathodic process, E^2_{pc} is the peak potential of the second cathodic process, and E^3_{pc} is the peak potential of the third cathodic process; E^1_{pa} is the peak potential of the first anodic process, and E^2_{pa} is the peak potential of the second anodic process.

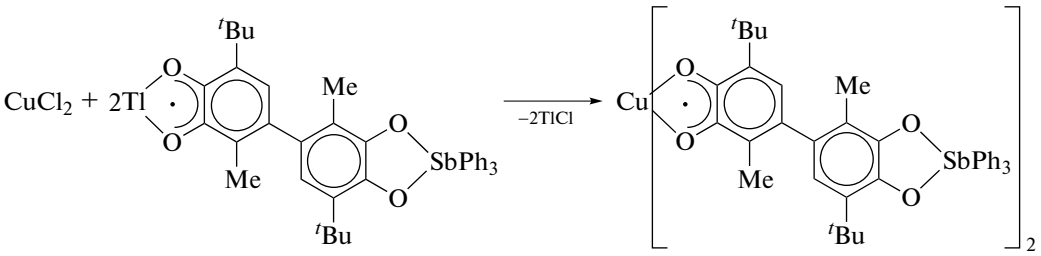

$Tl^{I}(SQ\text{-}Cat)SbPh_3$ $Cu^{II}[(SQ\text{-}Cat)SbPh_3]_2$ (**II**)

Scheme 2.

Complex **II** was isolated as a finely crystalline powder characterized by the data of IR spectroscopy, EPR spectroscopy, and elemental analysis. The IR spectrum of complex **II** exhibits absorption bands of stretching vibrations of the ordinary and one-and-half C–O bonds (1245, 1302, and 1450 cm^{-1}) and has no bands corresponding to the C=O vibrations of the carbonyl groups (1660 cm^{-1}).

The static magnetic susceptibility was measured for the obtained sample of complex **II**. The temperature dependence of μ_{eff} of the copper complex is shown in Fig. 2.

The effective magnetic moment at 300 K is 2.28 μ_B and decreases smoothly with decreasing temperature to 1.79 μ_B at 180 K. For the further temperature decrease to 25 K, μ_{eff} remains almost unchanged and equal to 1.68–1.78 μ_B. In the low-temperature range, complex **II** demonstrates a sharp decrease in μ_{eff} caused by a weak intermolecular exchange of the antiferromagnetic character. It follows from an analysis that the high-temperature value is substantially lower than the value expected for the system containing three noninteracting electrons (one electron on the copper atom and one on each SQ ligand), and the low-temperature values insignificantly differ from μ_{eff} for one unpaired electron [37].

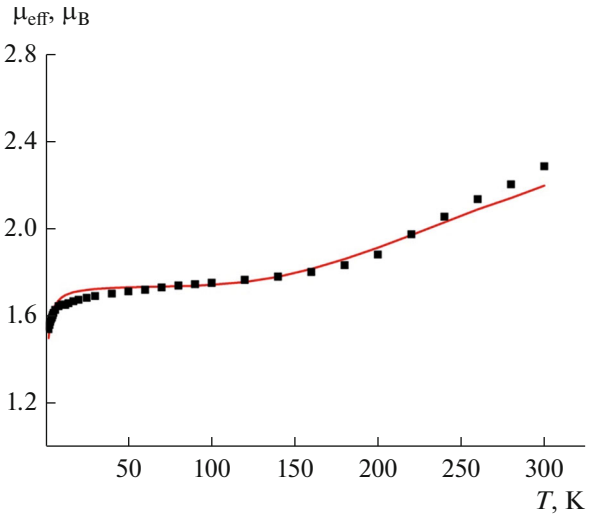

Fig. 2. Temperature dependence of the effective magnetic moment for complex **II** (μ_{calc} is shown by solid line).

The exchange interaction parameters in copper complex **II** were determined using the model for the system containing three exchange-bound spin centers (Scheme 3) using the Hamiltonian $H = -2J(S_1S_2 + S_2S_3) \times 2J_1S_1S_3$, where $S_1 = S_3 = 1/2$ are the spins of the semiquinone ligands, and S_2 is the spin of the paramagnetic metal ion ($S_2 = 1/2$ for Cu^{2+} ion) with allowance for the intermolecular exchange interaction (zJ) in the molecular field approximation.

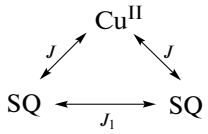

Scheme 3.

A satisfactory reproduction of the experimental data $\mu_{eff}(T)$ was obtained at the following parameters: $g_{SQ} = 2.0$ (fixed), $g_{Cu} = 2.01$, J(SQ-Cu) = –157 cm^{-1}, J(SQ-SQ) = J_1 = –10.0 cm^{-1}, zJ = –1.8 cm^{-1}, TIP = 0.0, and $R^2 = 7.7 \times 10^{-4}$.

$$R^2 = \frac{\Sigma\left(\chi_M T_{calc} - \chi_M T_{exp}\right)^2}{\Sigma\left(\chi_M T_{exp}\right)^2}.$$

The theoretical curve $\mu_{eff}(T)$ corresponding to these parameters is presented in Fig. 2 (solid line).

The obtained results are well consistent with the data of EPR spectroscopy. The EPR spectrum of complex **II** in the solid state is presented in Fig. 3. Thus, the spectral data suggest that the unpaired electron is localized on the organic ligand rather than on the copper(II) atom.

Similar examples of changing the magnetic and spectral properties of the copper(II) complexes with the redox-active radical ligands are known from the literature. For example, copper(II) bis-*o*-iminosemiquinolate based on 4,6-di-*tert*-butyl-2-(2-methylselenophenyl)aminophenol $Cu(ISQ\text{-}SeMe)_2$ was described [38]. The spectral and magnetic measurements showed that this complex has the doublet spin

state (S = 1/2) with the unpaired electron on the organic ligand. The EPR spectral parameters in the solid state at a lowered temperature for this complex are as follows: $g_1 = 2.012$, $g_2 = 2.006$, and $g_3 = 1.998$ ($g_{av} = 2.005$). The excited state with the spin $S = 3/2$ (quadruplet state) is observed for the complex with increasing temperature. These features of the magnetic and EPR spectral behavior of the copper(II) complex are explained by the distortion of the coordination sphere of the copper atom due to weak interactions between the selenium-containing lateral group and central copper atom. Owing to this, a certain angle is formed between the planes of the *o*-iminosemiquinone ligands and the character and value of the exchange metal–ligand and ligand–ligand magnetic interactions change. A similar situation is also observed for the PhSe-containing analogue $Cu^{II}(ISQ\text{-}SePh)_2$ [39]. The magnetic exchange parameters calculated for this copper complex are $J = -64.0$ cm^{-1} and $J' = -23.0$ cm^{-1} ($g_{Cu(II)} = 2.03$, $g_R = 2.00$). The EPR spectrum of the complex is characterized by a weaker anisotropy and the values of the g factor lower than 2 (1.964, 1.992, 1.992, g_{av} = 1.983). The authors concluded about the ligand-centered character of the unpaired electron in the doublet ground spin state of this complex. Later [40, 41] these research groups studied a series of similar copper(II) complexes for which different values of magnetic exchanges were observed depending on the molecular structure and the presence or absence of additional interactions with the central copper atom. In some cases, the distortions of the coordination node of copper(II) in the complexes are not related to additional interactions of the functional groups in the lateral units of the ligands with the copper atom but are determined by steric reasons, the bent structure of the ligands, etc. [42].

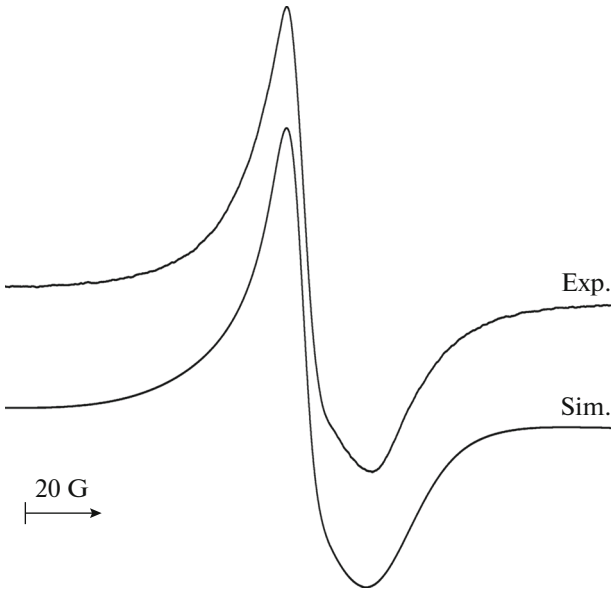

Fig. 3. EPR spectrum of copper complex **II** in a THF solution (298 K).

As mentioned above, a specific feature of *o*-quinones is their possibility to form several stable forms in complexes with metals. In the recent time, a tendency to study the complexes, where *o*-quinones act as neutral ligands, is observed in the coordination chemistry [43]. Similar complexes make it possible to obtain new properties in reactions of activating complexation [44]. The synthesis of the stable *o*-quinone complex with zinc iodide was described [43]. For the targeted preparation of the zinc complex with the neutral antimony-containing ligand (Q-Cat)$SbPh_3$, the reaction of the latter with zinc iodide in a toluene solution was performed (Scheme 4).

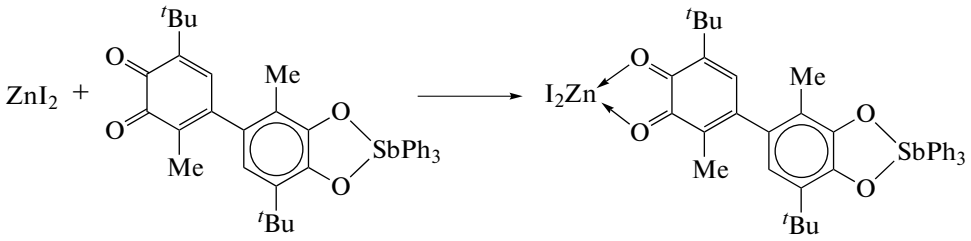

Scheme 4.

This reaction is accompanied by a sharp change in the color from vinous to violet and precipitation of finely crystalline product **III**. The IR spectrum of the isolated product exhibits the bands characteristic of the metal catecholate complexes in a range of 1200–1300 cm^{-1}, and the band corresponding to the ν(C=O) vibrations is observed at 1605 cm^{-1}. However, the intense bands corresponding to vibrations of the one-and-half C–O bonds are observed in a range of 1450–1480 cm^{-1}. The ^{1}H NMR spectrum contains signals from the protons of two *tert*-butyl groups with different linewidths and from the protons of the phenyl substituents at the antimony atom, but the signals from the protons in position 5 and the methyl groups are sig-

nificantly broadened. The synthesized sample also exhibits an impurity anisotropic EPR spectrum in the solid state. It was assumed by an analysis of the obtained results that the formation of molecular complex **III** enhanced the acceptor properties of *o*-quinone, which allowed the further redox transformations to occur (Scheme 5). This reaction occurs more efficiently in polar solvents.

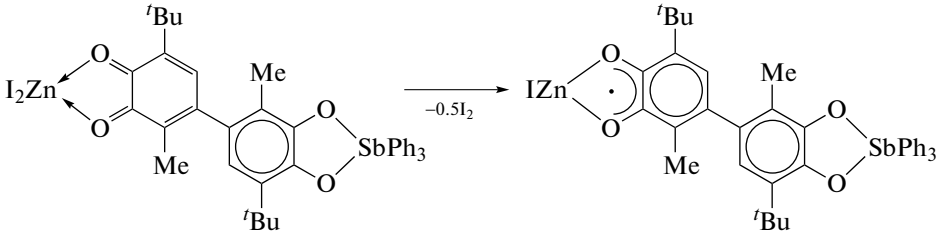

$I_2Zn(Q\text{-}Cat)SbPh_3$ (**III**) $IZn(SQ\text{-}Cat)SbPh_3$ (**IV**)

Scheme 5.

Complex **IV** was isolated from the mother liquor after the separation of complex **III**. The isotropic EPR spectrum of complex **IV** detected in a THF solution at room temperature (Fig. 4) represents a triplet of multiplets with $g_i = 2.0039$.

The EPR spectrum was simulated using the Easyspin 5.2.25 program package. The hyperfine structure is caused by the hyperfine interaction of the unpaired electron with the proton in position 5 of the aromatic ring of the *o*-benzosemiquinone fragment with the HFC constant $a_i(1^1H) = 3.23$ G and with the protons of two nonequivalent methyl groups (one CH_3 group in the *o*-semiquinone fragment, and the second CH_3 group in the catecholate fragment) with the HFC constants $a_i(3^1H) = 0.64$ G and $a_i(3^1H) = 0.29$ G, respectively. The parameters of this spectrum are close to the EPR parameters of similar complexes of the general type $M(SQ\text{-}Cat)SbPh_3$ described previously [24].

The electronic structure of complex **III** was additionally studied by quantum chemical calculations using the density functional theory (DFT). The calculations were performed at the B3LYP/DGDZVP level.

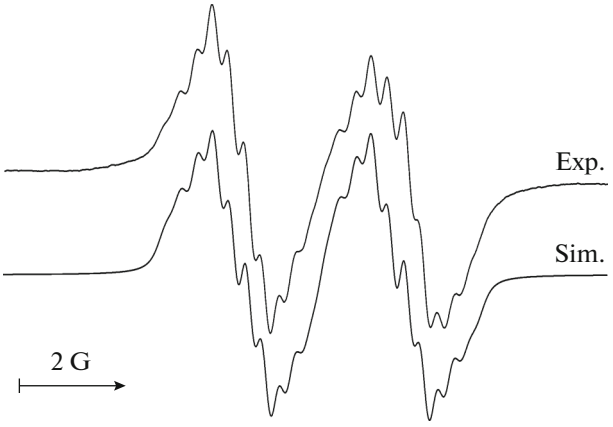

Fig. 4. Isotropic EPR spectrum of complex **IV** in THF (298 K).

According to the calculation data, the highest occupied molecular orbital (HOMO −5.8 eV) is mainly localized on the iodide anions (Fig. 5), and the lowly-lying HOMO-1 (−6.07 eV) is predominantly localized on the catecholate ligand (Fig. 5).

The lowest unoccupied molecular orbital (LUMO −4.32 eV) is predominantly localized on the quinone fragment (Fig. 5). A comparison of the frontier orbitals of complex **III** and initial antimony quinone-catecholate (HOMO −5.49 eV, LUMO −3.13 eV) has shown that the coordination with zinc iodide insignificantly decreases the HOMO but substantially increases the oxidative ability of the complex strongly decreasing the LUMO. The obtained data are well consistent with the data of UV spectroscopy, according to which the intense absorption band with a maximum at 910 nm and a molar absorption coefficient of 1×10^4 L/mol cm is observed in the near-IR range (Fig. 6).

The electronic transition energy at the absorption band maximum corresponds to ~30 kcal/mol. The dependences of the spectra on the concentration and temperature were additionally studied. It is shown that the Bouguer–Lambert–Beer law is fulfilled at room temperature in a range of the applied concentrations in dichloromethane with the consecutive dilution of the solution by two and three times, indicating the absorption of a single molecular system. As the temperature of the sample decreased from 20 to −30°C, the intensity of the band with a maximum at 910 nm increased by 30% (from 0.4 to 0.6 *A*) with the simultaneous shift of the maximum to 930 nm, which is characteristic of charge-transfer bands. It should be mentioned that this absorption band intensity decreases insignificantly and significantly when the spectra are recorded in dibromomethane and carbon tetrachloride, respectively, while this band is absent in such solvents as THF, acetonitrile, toluene, and chloroform at the same concentrations.

The electrochemical behavior of complex **III** is rather diverse (Fig. 7), and its transformations proceed as shown in Scheme 6.

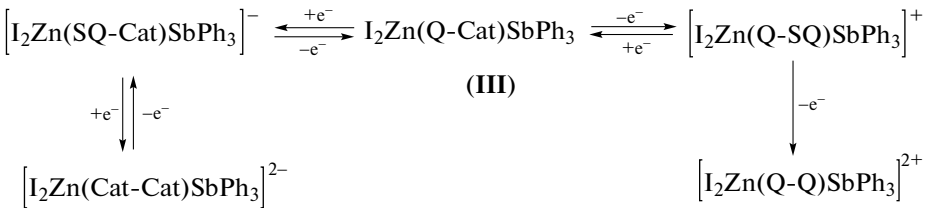

Scheme 6

The electrochemical behavior of compound **III** is characterized by the presence of two quasi-reversible reduction peaks at +0.43 and –0.49 V (Table 1) corresponding to the transformation of the SQ/Q and SQ/Cat fragments of the ligand. The coordination of the Lewis acid to the *o*-quinoid group results in a significant shift of the first reduction potential to the anodic range, which is due to the acceptor influence of ZnI_2. A similar behavior has previously been observed for the 3,6-di-*tert*-butyl-*o*-benzoquinone derivatives bearing coordinated $ZnBr_2$ [44], and the potentials of the redox transitions SQ/Q and SQ/Cat were fixed at positive values. In this case, the presence of the donor catecholate metallocycle partially compensates the acceptor influence of ZnI_2 and, hence, the first redox potential is observed at 0.43 V. The anodic range contains two weakly separated oxidation peaks (E_p^{ox1} = 0.85 and E_p^{ox2} = 0.96 V), which can be assigned to the transformation of the catecholate fragment into the corresponding *o*-quinone. It is most likely that no decoordination of ZnI_2 occurs, since the oxidation potentials would be identical to those obtained earlier form (Q-Cat)$SbPh_3$ (1.10 and 1.40 V).

Thus, the following heterometallic complexes were synthesized on the basis of triphenylantimony(V) quinone-catecholate: chromium(III) tris-*o*-semiquinolate $Cr^{III}[(SQ\text{-}Cat)SbPh_3]_3$, copper(II) bis-*o*-semiquinolate $Cu^{II}[(SQ\text{-}Cat)SbPh_3]_2$, zinc complexes with the neutral coordinated *o*-quinone ligand

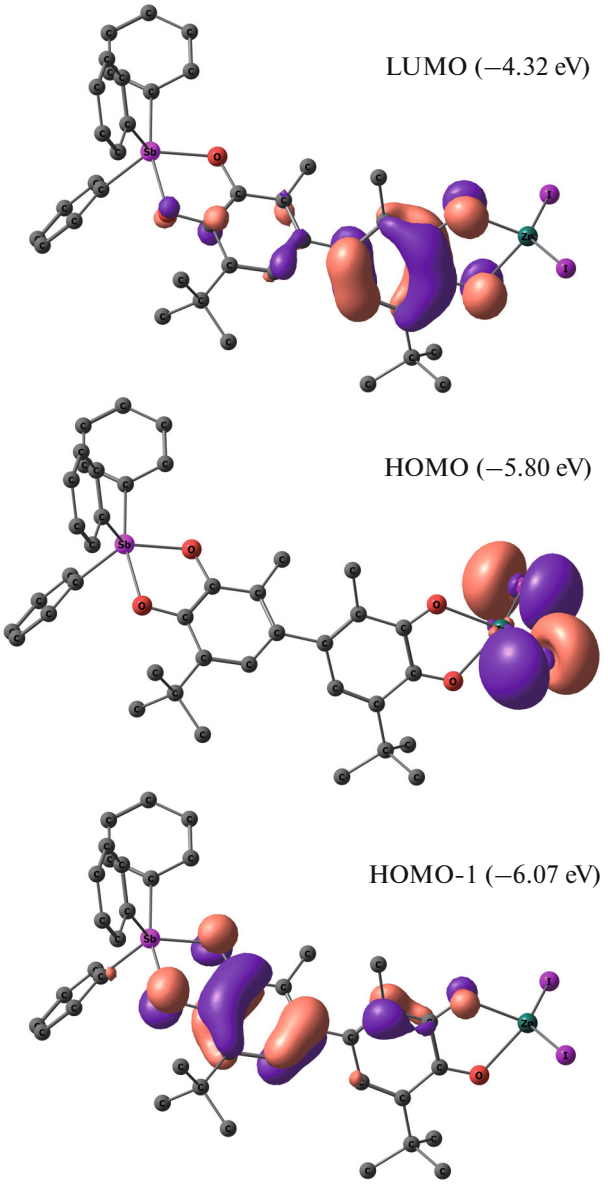

Fig. 5. Frontier orbitals in complex **III** calculated by the DFT method.

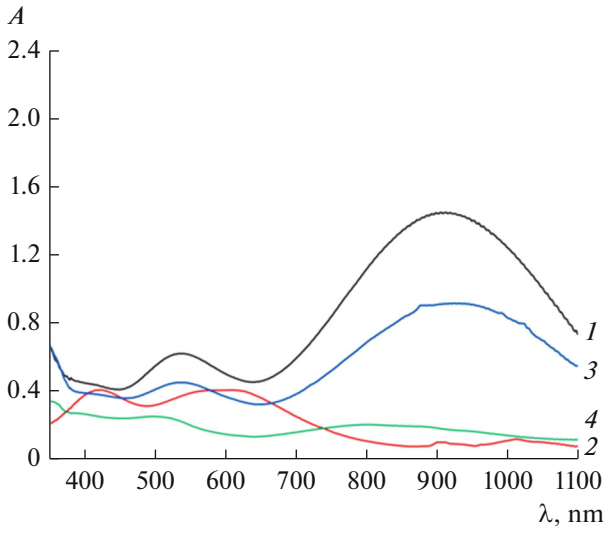

Fig. 6. Electronic absorption spectra of solutions of complex **III** in (*1*) CH_2Cl_2, (*2*) $CHCl_3$, (*3*) CH_2Br_2, and (*4*) CCl_4; $c = 1 \times 10^{-4}$ mol/L, $l = 1$ cm.

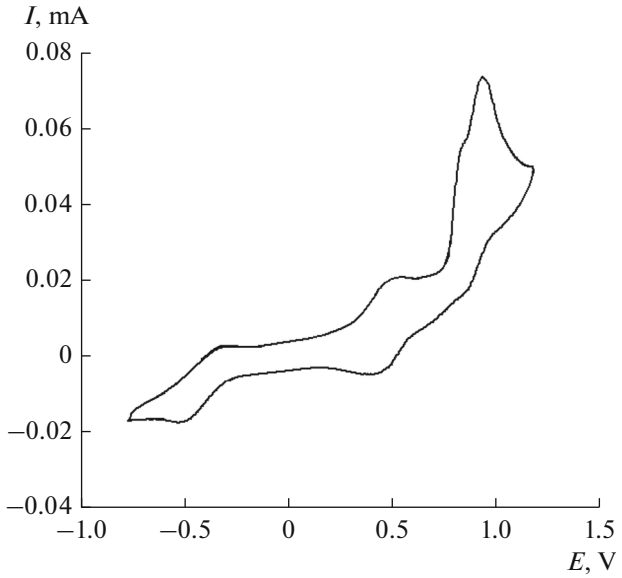

Fig. 7. CV curve of complex **III** at the potential sweep from −0.8 to 1.2 V (CH_2Cl_2, GC anode, $c = 0.002–0.003$ mol/L, 0.15 M NBu_4ClO_4, Ag/AgCl/KCl(sat.)).

$I_2Zn(Q\text{-}Cat)SbPh_3$, and iodozinc mono-*o*-semiquinolate $IZn(SQ\text{-}Cat)SbPh_3$. The formation of the monoreduced and monooxidized forms of the chromium(III) complex was detected by EPR spectroscopy: chromium(III) bis-*o*-semiquinolate catecholate $[Cr^{III}[(Cat\text{-}Cat)SbPh_3][(SQ\text{-}Cat)SbPh_3]_2]^-$ and chromium(III) *o*-quinone-bis-*o*-semiquinolate $[Cr^{III}[(Q\text{-}Cat)SbPh_3][(SQ\text{-}Cat)SbPh_3]_2]^+$, respectively. The copper(II) complex $Cu^{II}[(SQ\text{-}Cat)SbPh_3]_2$ has the doublet ground spin state with the unpaired electron on the ligand caused by the antiferromagnetic metal–ligand exchange ($J(SQ\text{-}Cu) = -157$ cm^{-1}, $J(SQ\text{-}SQ) = -10.0$ cm^{-1}). The oxidation ability of triphenylantimony(V) *o*-quinone-catecholate in the neutral complex with zinc iodide increases considerably (the first oxidation potential of Q/SQ increases from −0.45 V for $(Q\text{-}Cat)SbPh_3$) to 0.43 V (vs. Ag/AgCl/KCl(sat.)), and this complex can oxidize the iodide anion in the complex to elemental iodine with the formation of the paramagnetic *o*-semiquinone complex $IZn(SQ\text{-}Cat)SbPh_3$.

ACKNOWLEDGMENTS

The authors are grateful to A.S. Bogomyakov (International Tomography Center, Siberian Branch, Russian Academy of Sciences, Novosibirsk, Russia) for magnetochemical studies and A.V. Piskunov (Razuvaev Institute of Organometallic Chemistry, Russian Academy of Sciences, Nizhny Novgorod, Russia) for quantum chemical calculations. This work was carried out in terms of state assignment of the Razuvaev Institute of Organometallic Chemistry (Russian Academy of Sciences) using the equipment of the Analytical Center for Collective Use of the Razuvaev Institute of Organometallic Chemistry (Russian Academy of Sciences).

FUNDING

The study was carried out with the financial support of the Federal objective program "Research and development in priority directions of advancement of science and technology complex of Russia for 2014–2020" (Unique project identifier is RFMEFI62120X0040).

CONFLICT OF INTEREST

The authors declare that they have no conflict of interest.

REFERENCES

1. Adams, R.D. and Cotton, F.A., *Catalysis by Di- and Polynuclear Metal Cluster Complexes*, Wiley-VCH, 1998, p. 283.
2. Appel, A.M., Bercaw, J.E., Bocarsly, A.B., et al., *Chem. Rev.*, 2013, vol. 113, p. 6621.
3. Buchwalter, P., Rosé, J., and Braunstein, P., *Chem. Rev.*, 2015, vol. 115, p. 28.
4. Karkas, M.D., Verho, O., Johnston, E.V., and Akermark, B., *Chem. Rev.*, 2014, vol. 114, p. 11863.
5. Lee, S.C., Lo, W., and Holm, R.H., *Chem. Rev.*, 2014, vol. 114, p. 3579.
6. Tard, C. and Pickett, C.J., *Chem. Rev.*, 2009, p. 2245.
7. Nam, W., Lee, Y.M., and Fukuzumi, S., *Acc. Chem. Res.*, 2014, vol. 47, p. 1146.
8. Starikov, A.G., Starikova, A.A., Minyaev, R.M., et al., *Chem. Phys. Lett.*, 2020, vol. 740, p. 137073.
9. Albold, U., Hoyer, C., Neuman, N.I., et al., *Inorg. Chem.*, 2019, vol. 58, p. 3754.
10. Starikova, A.A., Metelitsa, E.A., and Minkin, V.I., *Russ. J. Coord. Chem.*, 2019, vol. 45, p. 411. https://doi.org/10.1134/S1070328419060095
11. Starikova, A.A. and Minkin, V.I., *Mendeleev Commun.*, 2016, vol. 26, p. 423.
12. Klementieva, S.V., Kuropatov, V.A., Fukin, G.K., et al., *Z. Anorg. Allg. Chem.*, 2011, vol. 637, p. 232.
13. Kuropatov, V., Klementieva, S., Fukin, G., et al., *Tetrahedron*, 2010, vol. 66, p. 7605.
14. Poddel'sky, A.I., Piskunov, A.V., Druzhkov, N.O., et al., *Z. Anorg. Allg. Chem.*, 2009, vol. 635, p. 2563.
15. Shultz, D.A., Fico, R.M., Jr., Bodnar, S.H., et al., *J. Am. Chem. Soc.*, 2003, vol. 125, p. 11761.
16. Caneschi, A., Dei, A., Mussari, C.P., et al., *Inorg. Chem.*, 2002, vol. 41, p. 1086.
17. Poddel'sky, A.I., Cherkasov, V.K., Bubnov, M.P., et al., *J. Organomet. Chem.*, 2005, vol. 690, p. 145.
18. Abakumov, G.A., Poddel'sky, A.I., Bubnov, M.P., et al., *Inorg. Chim. Acta*, 2005, vol. 358, p. 3829.
19. Smolyaninov, I.V., Antonova, N.A., Poddel'sky, A.I., et al., *J. Organomet. Chem.*, 2011, vol. 696, p. 2611.

20. Ilyakina, E.V., Poddel'sky, A.I., Piskunov, A.V., and Somov, N.V., *Inorg. Chim. Acta*, 2012, vol. 380, p. 57.
21. Ilyakina, E.V., Poddel'sky, A.I., Cherkasov, V.K., and Abakumov, G.A., *Mendeleev Commun.*, 2012, vol. 22, p. 208.
22. Kuropatov, V.A., Klementieva, S.V., Poddel'sky, A.I., et al., *Russ. Chem. Bull.*, 2010, vol. 59, p. 1698.
23. Piskunov, A.V., Cherkasov, V.K., Druzhkov, N.O., et al., *Russ. Chem. Bull.*, 2005, vol. 54, p. 1627.
24. Cherkasov, V.K., Grunova, E.V., and Abakumov, G.A., *Russ. Chem. Bull.*, 2005, vol. 54, p. 2067.
25. Bencini, A., Daul, C.A., Dei, A., et al., *Inorg. Chem.*, 2001, vol. 40, p. 1582.
26. Abakumov, G.A., Nevodchikov, V.I., Druzhkov, N.O., et al., *Russ. Chem. Bull.*, 1997, vol. 46, p. 771.
27. Cherkasov, V.K., Grunova, E.V., Poddel'sky, A.I., et al., *J. Organomet. Chem.*, 2005, vol. 690, p. 1273.
28. Gordon, A. and Ford, R., *The Chemist's Companion: A Handbook of Practical Data, Techniques, and References*, New York: Wiley, 1972.
29. Frisch, M.J., Trucks, G.W., Schlegel, H.B., et al., *Gaussian 09 (revision E.01)*, Wallingford: Gaussian Inc., 2013.
30. Litvinenko, A.S., Mikhaleva, E.A., Kolotilov, S.V., and Pavlishchuk, V.V., *Theor. Experiment. Chem.*, 2011, vol. 46, p. 422.
31. Buchanan, R.M., Kessel, S.L., Downs, H.H., et al., *J. Am. Chem. Soc.*, 1978, vol. 100, p. 7894.
32. Buchanan, R.M., Downs, H.H., Shorthill, W.B., et al., *J. Am. Chem. Soc.*, 1978, vol. 100, p. 4318.
33. Rodriguez, J.H., Wheeler, D.E., and McCusker, J.K., *J. Am. Chem. Soc.*, 1998, vol. 120, p. 12051.
34. Pierpont, C.G. and Downs, H.H., *J. Am. Chem. Soc.*, 1976, vol. 98, p. 4834.
35. Chang, H.-Ch., Ishii, T., Kondo, M., and Kitagawa, S., *Dalton Trans.*, 1999, p. 2467.
36. Sofen, S.R., Ware, D.C., Cooper, S.R., and Raymond, K.N., *Inorg. Chem.*, 1979, vol. 18, p. 234.
37. Abakumov, G.A., Cherkasov, V.K., Bubnov, M.P., et al., *Izv. Akad. Nauk, Ser. Khim.*, 1992, vol. 10, p. 2315.
38. Bubrin, M., Paretzki, A., Hubner, R., et al., *Z. Anorg. Allg. Chem.*, 2017, vol. 643, p. 1621.
39. Rakshit, R., Ghorai, S., Biswas, S., and Mukherjee, C., *Inorg. Chem.*, 2014, vol. 53, p. 3333.
40. Paretzki, A., Hubner, R., Ye, Sh., et al., *J. Material. Chem.*, 2015, vol. 3, p. 4801.
41. Mondal, M.K. and Mukherjee, C., *Dalton Trans.*, 2016, vol. 45, p. 13532.
42. Kaim, W., *Dalton Trans.*, 2003, p. 761.
43. Abakumov, G.A., Cherkasov, V.K., Piskunov A.V., et al., *Dokl. Chem.*, 2009, vol. 427, p. 330.
44. Abakumov, G.A., Cherkasov, V.K., Piskunov, A.V., et al., *Dokl. Chem.*, 2010, vol. 434, p. 344.

Translated by E. Yablonskaya